Complementary Use of Model-Free and Modelistic Methods in the Analysis of Solid-State Kinetics

Ammar Khawam* and Douglas R. Flanagan

Division of Pharmaceutics, College of Pharmacy, University of Iowa, 115 South Grand Avenue, Iowa City, Iowa 52242

Received: February 2, 2005; In Final Form: March 29, 2005

There are many methods for analyzing solid-state kinetic data. They are generally grouped into two categories, model-fitting and isoconversional (model-free) methods. Historically, model-fitting methods were widely used because of their ability to directly determine the kinetic triplet (i.e., frequency factor [*A*], activation energy [E_a], and model). However, these methods suffer from several problems among which is their inability to uniquely determine the reaction model. This has led to the decline of these methods in favor of isoconversional methods that evaluate kinetics without modelistic assumptions. This work proposes an approach that combines the power of isoconversional methods with model-fitting methods. It is based on using isoconversional methods instead of traditional statistical fitting methods to select the reaction model. Once a reaction model has been selected, the activation energy and frequency factor can be determined for that model. This approach was investigated for simulated and real experimental data for desolvation reactions of sulfameter solvates.

1. Introduction

Many methods have been developed for studying solid-state kinetic data. These methods can be classified according to the experimental conditions selected and the mathematical analysis performed. Experimentally, either isothermal or nonisothermal methods are employed. The mathematical approaches employed can be divided into model-fitting and isoconversional (model-free) methods. Model-fitting methods were among the first and most popular methods to be used in evaluating solid-state kinetics, especially for nonisothermal experiments. The popularity of these methods has recently declined in favor of isoconversional methods which can compute kinetic parameters without modelistic assumptions. However, these methods, like the model-fitting methods, have some limitations.[1,2]

Results obtained from different mathematical analysis methods have been viewed as conflicting rather than complementary. In a recent paper by Zhou and Grant,[3] it was demonstrated that model-fitting of simulated isothermal kinetic data gave little variation in activation energy (E_a) with different models. On the other hand, these same authors showed that simulated nonisothermal data gave wide variation in E_a depending on the model.

Selection of the best model for experimental data is problematic because a statistical fit parameter (i.e., r^2) may be quite high for a number of fitted models.[4] The aim of this work is to show the utility of a model-free method to obtain activation energy (E_a) and a modelistic approach to obtain frequency factor (A). We feel that such an approach gives the highest probability of selecting the most accurate kinetic triplet (A, E_a, and model). The kinetic triplet is essential for accurate kinetic description of any solid-state reaction since the reaction rate expression (eq 10) requires all three. If only one or two of the triplet are known, an incomplete kinetic picture is generated.[5−7] Just as in homogeneous phase kinetics, obtaining all kinetic parameters for a solid-state reaction is essential for understanding reaction dynamics. In this work, we will demonstrate how such a complete analysis can be accomplished using simulated kinetic data and real data for a desolvation reaction.

1.1. Rate Laws and Kinetic Analysis. The rate of a solid-state reaction can be generally described by,

$$\frac{d\alpha}{dt} = k\, f(\alpha) \tag{1}$$

where k is the reaction rate constant, $f(\alpha)$ is the reaction model, and α is the conversion fraction.

Integrating the above equation gives the integral rate law,

$$g(\alpha) = kt \tag{2}$$

where, $g(\alpha)$ is the integral degradation model.

The temperature dependence of the rate constant is described by the Arrhenius equation,[8]

$$k = Ae^{-E_a/RT} \tag{3}$$

where A is the preexponential (frequency) factor, E_a is the activation energy, T is the absolute temperature, and R is the gas constant.

Substituting eq 3 in the above rate expressions gives,

$$\frac{d\alpha}{dt} = Ae^{-E_a/RT} f(\alpha) \tag{4}$$

and

$$g(\alpha) = Ae^{-E_a/RT}t \tag{5}$$

Several reaction models are listed in Table 1.

The above rate expressions can be transformed into nonisothermal rate expressions describing reaction rates as a function

* Corresponding author. E-mail: ammar-khawam@uiowa.edu. Phone: (319) 335-8819. Fax: (319) 335-9349.

10.1021/jp050589u CCC: $30.25
Published on Web 04/21/2005

TABLE 1: Solid-State Rate Expressions for Different Reaction Models

model	differential form $f(\alpha) = (1/k)\,(d\alpha/dt)$	integral form $g(\alpha) = kt$
	nucleation models	
power law (P2)	$2\alpha^{(1/2)}$	$\alpha^{(1/2)}$
power law (P3)	$3\alpha^{(2/3)}$	$\alpha^{(1/3)}$
power law (P4)	$4\alpha^{(3/4)}$	$\alpha^{(1/4)}$
Avarami−Erofe'ev (A2)	$2(1-\alpha)[-\ln(1-\alpha)]^{1/2}$	$[-\ln(1-\alpha)]^{1/2}$
Avarami−Erofe'ev (A3)	$3(1-\alpha)[-\ln(1-\alpha)]^{2/3}$	$[-\ln(1-\alpha)]^{1/3}$
Avarami−Erofe'ev (A4)	$4(1-\alpha)[-\ln(1-\alpha)]^{3/4}$	$[-\ln(1-\alpha)]^{1/4}$
	geometrical contraction models	
contracting area (R2)	$2(1-\alpha)^{1/2}$	$[1-(1-\alpha)^{1/2}]$
contracting volume (R3)	$3(1-\alpha)^{2/3}$	$[1-(1-\alpha)^{1/3}]$
	diffusion models	
1-D diffusion (D1)	$1/2\alpha$	α^2
2-D diffusion (D2)	$[-\ln(1-\alpha)]^{-1}$	$[(1-\alpha)\ln(1-\alpha)]+\alpha$
3-D diffusion−Jander eq (D3)	$3(1-\alpha)^{2/3}/2(1-(1-\alpha)^{1/3})$	$[1-(1-\alpha)^{1/3}]^2$
Ginstling−Brounshtein (D4)	$(3/2((1-\alpha)^{-1/3}-1)$	$1-(2\alpha/3)-(1-\alpha)^{2/3}$
	reaction-order models	
zero-order (F0/R1)	1	α
first-order (F1)	$(1-\alpha)$	$-\ln(1-\alpha)$
second-order (F2)	$(1-\alpha)^2$	$(1-\alpha)^{-1}-1$
third-order (F3)	$(1-\alpha)^3$	$0.5[(1-\alpha)^{-2}-1]$

of temperature at a constant heating rate by utilizing the following equation,

$$\frac{d\alpha}{dT} = \frac{d\alpha}{dt}\cdot\frac{dt}{dT} \tag{6}$$

where $d\alpha/dT$ is the nonisothermal reaction rate, $d\alpha/dt$ is the isothermal reaction rate, and dT/dt is the heating rate (β).

Substituting eq 4 in the above equation gives the differential form of the nonisothermal rate law,

$$\frac{d\alpha}{dT} = \frac{A}{\beta}e^{-E_a/RT} f(\alpha) \tag{7}$$

Upon integration eq 7 gives,

$$g(\alpha) = \frac{A}{\beta}\int_0^T e^{-E_a/RT}\,dT \tag{8}$$

If E_a/RT is replaced by "x" and the integration limits are transformed, the above equation becomes,

$$g(\alpha) = \frac{AE_a}{\beta R}\int_x^\infty \frac{e^{-x}}{x^2}\,dx \tag{9}$$

This is written as,

$$g(\alpha) = \frac{AE_a}{\beta R}\,p(x) \tag{10}$$

where, $p(x)$ is the exponential integral.

The exponential integral ($p(x)$) has no analytic solution,[9] but has many approximations.[9−13]

Kinetic parameters can be obtained from isothermal and nonisothermal rate laws by both model-fitting and isoconversional methods.

In isothermal experiments, the conventional model-fitting method[1] involves two fits: the first determines the model that best fits the data (eq 2) while the second determines specific kinetic parameters such as the activation energy (E_a) and frequency factor (A), using the Arrhenius equation (eq 3). For nonisothermal experiments, model fitting involves fitting different models to α−temperature ($\alpha-T$) curves and simultaneously determining E_a and A.[4]

There are numerous nonisothermal model-fitting methods; one of the most popular is the Coats and Redfern method.[14,15] This method utilizes the asymptotic series expansion in approximating $p(x)$ (eq 10), producing the following equation,

$$\ln\frac{g(\alpha)}{T^2} = \ln\left(\frac{AR}{\beta E_a}\left[1-\left(\frac{2RT_{exp}}{E_a}\right)\right]\right) - \frac{E_a}{RT} \tag{11}$$

where T_{exp} is the mean experimental temperature.

Plotting the left-hand side (which includes the model $g(\alpha)$) of eq 11 versus $1/T$ gives E_a and A from the slope and intercept, respectively. The model that gives the best linear fit is selected as the model of choice.

The use of modelistic methods has been criticized in nonisothermal studies[6,16−20] because regression methods may lead to indistinguishable fits or mathematical expressions with high correlation because of the form of the equation. This casts serious doubt on using these methods to obtain mechanistic information (A, E_a, and model). Model-fitting problems are especially evident with the Coats and Redfern method in which the ordinate ($\ln(g(\alpha)/T^2)$) and abscissa ($1/T$) axes are correlated because of the form of each variable, which violates a basic assumption of linear regression.[21] As a result, all models would show relatively good fits (i.e. high r^2) even though they may be poor descriptors of the mechanism. Another problem with the Coats−Redfern method is that some models are indistinguishable. For example, the F1, A2, A3, and A4 models are indistinguishable when linear regression is performed as they all show very similar correlation coefficients.

Vyazovkin and Wight[20] reviewed several alternative nonstatistical approaches for model selection. These include using predictions of the activated complex to obtain the frequency factor, selecting a model from an isothermal experiment,[22] or choosing a reaction model from the extent of the reaction at the maximum reaction rate (α_{max}).[23] These approaches have not gained wide use. Therefore, Vyazovkin and Wight have recommended using isoconversional methods instead of modelistic approaches.

Isoconversional methods calculate E_a values at progressive degrees of conversion without modelistic assumptions. The standard isoconversional method[1] is an isothermal method that is based on taking the natural logarithm of eq 5 giving,

$$-\ln t = \ln\left(\frac{A}{g(\alpha)}\right) - \frac{E_a}{RT} \quad (12)$$

A plot of $-\ln t$ versus $1/T$ at each α yields E_a from the slope for that α without regard to a model.

The Vyazovkin isoconversional method[24] is a nonisothermal method that utilizes an accurate, nonlinear, Senum−Yang[13] approximation of $p(x)$ (eq 10), which leads to,

$$\Omega = \left|\sum_{i=1}^{n}\sum_{j\neq i}^{n}\frac{\beta_j I(E_{a\alpha},T_{\alpha i})}{\beta_i I(E_{a\alpha},T_{\alpha j})}\right| \quad (13)$$

where $I(E_{a\alpha},T_{\alpha i})$ is the exponential integral ($p(x)$) that results from heating rate β_i while $I(E_{a\alpha},T_{\alpha j})$ is the exponential integral from heating rate β_j. The 4th degree Senum−Yang approximation was chosen for our work. The activation energy (E_a) is the value that minimizes Ω in the above equation.

Despite concerns over use of model-fitting methods, these methods have the advantage of directly calculating E_a and A from a single nonisothermal kinetic run. This is not seen in isoconversional methods as they require multiple kinetic runs at different heating rates and do not allow direct calculation of A. An indirect method has been suggested [25] to calculate A for isoconversional methods; however, this procedure utilizes an artificial isokinetic relationship that is not fully supported theoretically.[26]

This work utilizes isoconversional methods to obtain E_a values which are compared to values obtained by modelistic methods. The most accurate model is assumed to be the one that produces an activation energy closest to that from the isoconversional analysis. This allows one to select models that might otherwise be indistinguishable based on quality of the regression fit alone. We demonstrate the utility of this approach by analyzing both simulated and experimental data.

Experimental data were obtained for the desolvation kinetics of a drug solvate. A solvate crystal form is one in which solvent molecules occupy specific positions within the crystal structure. Desolvation is a reaction involving the removal of solvent molecules from the crystalline solvate below its melting point.[27] The drug in these studies was sulfameter (see structure below), which is a long-acting sulfonamide used for the treatment of urinary tract infections.[28] Three sulfameter solvates (solvent structures below) were prepared with cyclic ethers and their desolvation kinetics followed by thermogravimetry (TGA).

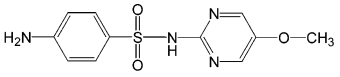

Sulfameter (5–methoxysulfadiazine)
mw – 280.3

Tetrahydrofuran
mw – 72.11

Dioxolane
mw – 74.08

Dioxane
mw – 88.11

2. Experimental Section

Simulated data were isothermally and nonisothermally generated and then analyzed, as described below. Sulfameter desolvation was followed nonisothermally by TGA. Isothermal calculation methods included the conventional model-fitting method (modelistic) and the standard isoconversional method (model-free).[1] Nonisothermal calculation methods included the Coats and Redfern method[14,15] (modelistic) in addition to Vyazovkin's method [24] (model-free).

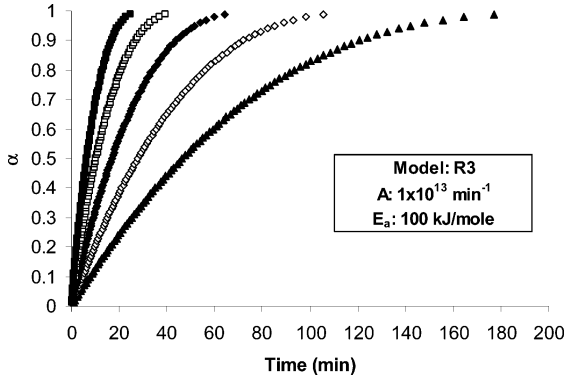

Figure 1. Simulations of α versus time for isothermal kinetic runs with 0.25% random error in time at (▲) 340, (◇) 345, (◆) 350, (□) 355, and (■) 360 K (simulation S1). The inset gives the simulation model, preexponential factor (A), and activation energy (E_a).

2.1. Data Simulation. A simple, one-step reaction (solid A producing solid B and gas C), according to the scheme below, was simulated.

$$A_{(s)} \rightarrow B_{(s)} + C_{(g)}$$

Isothermal simulations were generated with Microsoft Excel from the integral form of the rate law (eq 5). The simulation was done by calculating the time (t) for α values between 0.01 and 0.99 according to:

$$t = \frac{g(\alpha)}{Ae^{-E_a/RT}} \quad (14)$$

Values were assigned to the above parameters ($g(\alpha)$, E_a, A, and T) to calculate the time for each α. The isothermal simulation (S1) consisted of five isothermal (α−time) curves which were simulated at five temperatures (340, 345, 350, 355, and 360 K), using a contracting volume (R3) model ($g(\alpha) = [1 - (1 - \alpha)^{1/3}]$) with $A = 1 \times 10^{13}$ min^{-1} and $E_a = 100$ kJ/mol. A 0.25% random error in time was introduced to each curve in the simulation (Figure 1).

Nonisothermal data were simulated by calculating the temperature (T) for α values between 0.01 and 0.99 according to:

$$\Psi = \left|g(\alpha)\frac{\beta R}{AE_a} - p(x)\right| \quad (15)$$

Values were assigned to the above parameters ($g(\alpha)$, E_a, A, and β), and the exponential integral ($p(x)$) was approximated by the 3rd degree Senum−Yang approximation. Nonisothermal data were simulated with Microsoft Excel's Solver by finding the value of T at each α, which minimized Ψ in eq 15. The nonisothermal simulation (S2) consisted of five nonisothermal (α−T) curves which were simulated at five heating rates (1, 2, 4, 8, and 16 K/min), using the same kinetic parameters (model, E_a, and A) used for simulation S1. A 0.25% random error in temperature (°C) was introduced to each curve in the simulation (Figure 2).

2.2. Sulfameter Solvate Desolvation. Sulfameter was obtained from Sigma Chemical Co. (lot 107F0910), tetrahydrofuran and dioxane were obtained from Fisher Scientific (lots 031014 and 023029, respectively), while dioxolane was obtained from Aldrich Chemical Co. (lot LO14921KO). All chemicals were used as supplied. Solvates of sulfameter were prepared by recrystallizing sulfameter from the neat solvent. The prepared solvates were sieved and a particle size range of 355−710 μm was used for desolvation studies.

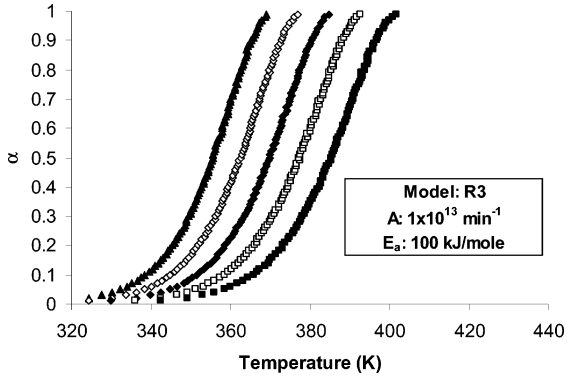

Figure 2. Simulated α-temperature plots with 0.25% random error in temperature (°C) for nonisothermal kinetic runs at (▲) 1, (◇) 2, (◆) 4, (□) 8, and (■) 16 K/min (simulation S2). The inset gives the simulation model, preexponential factor (A), and activation energy (E_a).

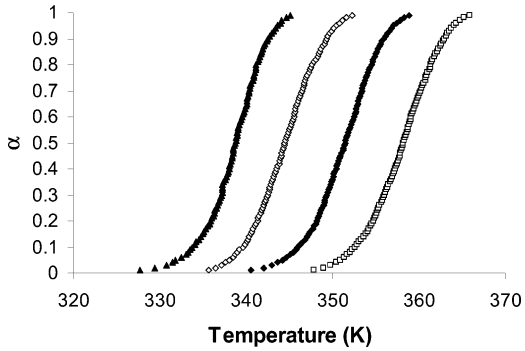

Figure 3. α versus temperature plots for the nonisothermal desolvation of sulfameter−tetrahydrofuran solvate at (▲) 0.95, (◇) 1.93, (◆) 3.86, and (□) 7.61 K/min.

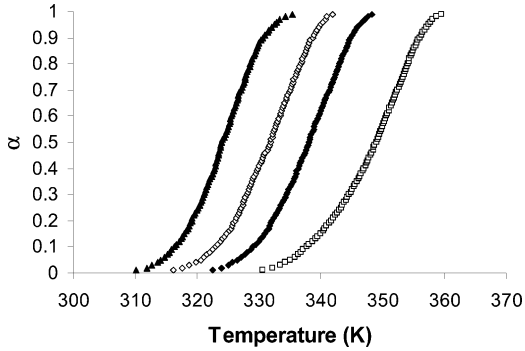

Figure 4. α versus temperature plots for the nonisothermal desolvation of sulfameter−dioxolane solvate at (▲) 0.96, (◇) 1.92, (◆) 3.80, and (□) 7.62 K/min.

Desolvation kinetics was followed nonisothermally by TGA, using a Perkin-Elmer TGA 7. The TGA temperature was calibrated by a two-point calibration method, using alumel and nickel. A flow of nitrogen gas of 40−50 mL/min was used as a purge. A sample of 2−4 mg of solvate was used for each kinetic run. Nonisothermal runs were performed at nominal heating rates of 1, 2, 4, and 8 K/min. The exact heating rate was obtained from the slope of the linear heating curve of the TGA run during the time period of significant weight loss.

2.3. Kinetic Analysis. Kinetic analysis of data was conducted by model-fitting and isoconversional methods. Simulated isothermal data were analyzed by the conventional model-fitting method and the standard isoconversional method while nonisothermal data were analyzed by the Coats−Redfern model-fitting method in addition to Vyazovkin's isoconversional method.

Model selection was done by means of an isoconversional-model (IM) plot in which a plot of E_a for each model, as calculated from the Coats−Redfern method, was plotted along with E_a calculated from Vyazovkin's isoconversional method as a function of α. The model for which E_a matched that from the isoconversional plot was selected as the model of choice.

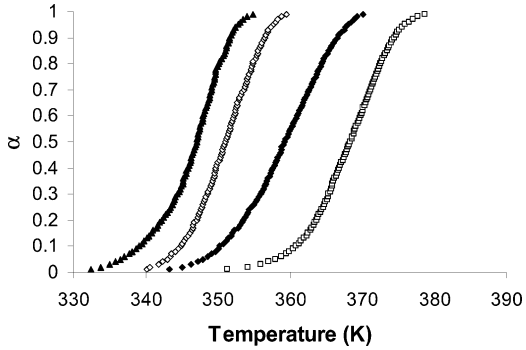

Figure 5. α versus temperature plots for the nonisothermal desolvation of sulfameter−dioxane solvate at (▲) 0.98, (◇) 1.99, (◆) 3.94, and (□) 7.71 K/min.

TABLE 2: Fitted Kinetic Parameters for Simulated Isothermal Data (S1), Using the Conventional Model-Fitting Method

model	A (min^{-1})	E_a (kJ/mol)	r^a
A2	2.40×10^{13}	100.05	0.9933
A3	1.66×10^{13}	100.06	0.9761
A4	1.28×10^{13}	100.06	0.9618
D1	1.58×10^{13}	100.05	0.9922
D2	1.36×10^{13}	100.05	0.9917
D3	6.56×10^{12}	100.04	0.9514
D4	3.87×10^{12}	100.05	0.9846
F1	4.88×10^{13}	100.05	0.9809
F2	4.10×10^{14}	100.04	0.6506
F3	1.13×10^{16}	100.04	0.4084
P2	1.14×10^{13}	100.06	0.9090
P3	8.99×10^{12}	100.07	0.8790
P4	7.38×10^{12}	100.07	0.8610
R1	1.49×10^{13}	100.06	0.9631
R2	1.25×10^{13}	100.05	0.9967
R3[b]	1.02×10^{13}	100.05	1.0000

[a] Correlation coefficient for $g(\alpha)$ vs t plot. [b] Best fit model.

2.4. Curve Reconstruction and Stability Prediction. TGA curves were reconstructed to verify that the most accurate kinetic triplet (A, E_a, and model) was selected by the isoconversional method for each heating rate (1, 2, 4, and 8 K/min).

The selected kinetic triplet was also used to predict the stability of each solvate at three different heating rates that were not used in the kinetic analysis. The exact heating rate was obtained from the slope of the linear heating curve of the TGA run during the time period of significant weight loss. Equation 15 was used to reconstruct/predict each curve.

3. Results and Discussion

Thermogravimetric results for sulfameter desolvation are shown in Figures 3−5. Gravimetric weight loss for these solvates showed a 1:1 drug−solvent ratio (~20.5%, 20.6%, and 24% w/w for tetrahydrofuran, dioxolane, and dioxane, respectively). Kinetic analysis for the simulated and real data sets is described below.

3.1. Simulated Data. Model-fitting methods produced several kinetic triplets (A, E_a, and model) for each simulation. The conventional model fitting results for simulation S1 are given in Table 2, while results obtained by the Coats−Redfern method for simulation S2 are in Table 3.

Isoconversional-model (IM) plots containing activation energies calculated by model-fitting along with that calculated from an isoconversional method are shown in Figures 6 and 7. IM

TABLE 3: Fitted Kinetic Parameters for Simulated Nonisothermal Data (S2), Using the Coats−Redfern Method[a]

model	A (min^{-1})	E_a (kJ/mol)	r
A2	4.18×10^{06}	52.21	−0.9970[c]
A3	5.46×10^{03}	32.80	−0.9967[c]
A4	1.86×10^{02}	23.10	−0.9963[c]
D1	2.06×10^{23}	171.44	−0.9924
D2	1.67×10^{25}	186.01	−0.9974[c]
D3	3.07×10^{27}	205.38	−0.9999[c]
D4	3.31×10^{25}	192.31	−0.9988[c]
F1	1.18×10^{15}	110.44	−0.9972[c]
F2	2.45×10^{21}	152.26	−0.9576
F3	1.69×10^{29}	204.49	−0.9059
P2	2.80×10^{04}	38.35	−0.9903
P3	1.82×10^{02}	23.56	−0.9883
P4	1.44×10^{01}	16.16	−0.9858
R1	6.78×10^{10}	82.71	−0.9918
R2	2.52×10^{12}	94.90	−0.9993[c]
R3[b]	9.02×10^{12}	99.68	−0.9999[c]

[a] Results averaged from five curves by taking the geometrical mean of A and E_a and arithmetic mean of r. [b] Model selected based on isoconversional-model (IM) plots. [c] Equivalent models based on goodness of fit.

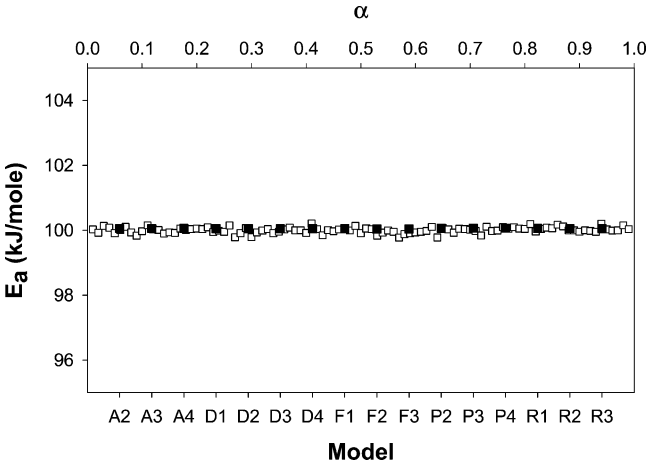

Figure 6. Isoconversional-model plot of activation energies for simulation S1 calculated by (■) the conventional model-fitting method and (□) the standard isoconversional method.

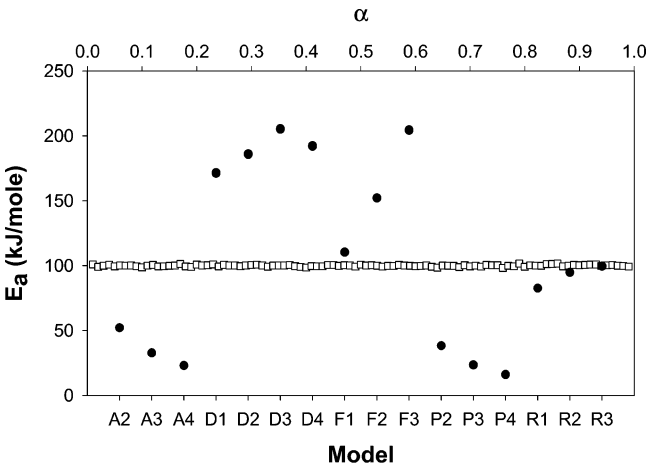

Figure 7. Isoconversional-model plot of activation energies for simulation S2 calculated by (●) Coats−Redfern's modelistic method and (□) Vyazovkin's isoconversional method.

plots of isothermal data (S1, Figure 6) show that no particular model can be selected because all models give comparable values of E_a (∼100 kJ/mol, Table 2). Previous reports have demonstrated similar constancy of E_a,[1,3,4,20] which is the reason that the desolvation reaction was not further studied isothermally.

TABLE 4: Fitted Kinetic Parameters for the Nonisothermal Desolvation of Sulfameter−Tetrahydrofuran Solvate, Using the Coats−Redfern Method[a]

model	A (min^{-1})	E_a (kJ/mol)	r
A2	3.12×10^{23}	159.64	−0.9916[c]
A3[b]	1.21×10^{15}	104.50	−0.9913[c]
A4	6.90×10^{10}	76.93	−0.9909[c]
D1	3.07×10^{71}	480.96	−0.9527
D2	1.17×10^{78}	525.89	−0.9665
D3	5.96×10^{86}	587.13	−0.9817
D4	2.84×10^{80}	545.76	−0.9721
F1	3.21×10^{48}	325.07	−0.9919[c]
F2	2.18×10^{69}	461.28	−0.9921[c]
F3	3.09×10^{95}	632.71	−0.9663
P2	5.11×10^{16}	115.90	−0.9493
P3	3.27×10^{10}	75.34	−0.9468
P4	2.41×10^{07}	55.06	−0.9442
R1	1.17×10^{35}	237.59	−0.9516
R2	4.09×10^{40}	275.58	−0.9746
R3	5.68×10^{42}	290.68	−0.9813

[a] Results averaged from five curves by taking the geometrical mean of A and E_a and arithmetic mean of r. [b] Model selected based on isoconversional-model (IM) plots. [c] Equivalent models based on goodness of fit.

TABLE 5: Fitted Kinetic Parameters for the Nonisothermal Desolvation of Sulfameter−Dioxolane Solvate, Using the Coats−Redfern Method[a]

model	A (min^{-1})	E_a (kJ/mol)	r
A2[b]	1.26×10^{13}	88.30	−0.9918[c]
A3	1.22×10^{08}	57.01	−0.9913[c]
A4	3.48×10^{05}	41.37	−0.9907[c]
D1	3.13×10^{41}	271.90	−0.9572
D2	1.98×10^{45}	297.26	−0.9704
D3	1.48×10^{50}	331.53	−0.9841
D4	2.75×10^{46}	308.40	−0.9756
F1	8.57×10^{27}	182.15	−0.9924[c]
F2	1.30×10^{40}	257.57	−0.9854
F3	2.23×10^{55}	352.29	−0.9544
P2	1.13×10^{09}	63.81	−0.9517
P3	2.22×10^{05}	40.68	−0.9475
P4	2.88×10^{03}	29.12	−0.9427
R1	9.27×10^{19}	133.17	−0.9555
R2	1.41×10^{23}	154.54	−0.9775
R3	2.22×10^{24}	162.98	−0.9836

[a] Results averaged from five curves by taking the geometrical mean of A and E_a and arithmetic mean of r. [b] Model selected based on isoconversional-model (IM) plots. [c] Equivalent models based on goodness of fit.

IM plots of nonisothermal data (S2, Figure 7) show that the R3 model is selected as the best model because E_a for R3, calculated by the Coats−Redfern method, is almost the same as that calculated by Vyazovkin's isoconversional method (∼99.7 kJ/mol, Table 3). If model selection is to be based on the correlation coefficient (r), no single model can be chosen because several models are equivalent (A2, A3, A4, D2, D3, D4, F1, R2, and R3) as indicated in Table 3. This shows that model selection based on IM plots is more appropriate than that using the correlation coefficient.

3.2. Sulfameter Desolvation. Several kinetic triplets were calculated from the Coats−Redfern model-fitting method for each solvate (Tables 4−6). Results based on curve fitting clearly show that using the correlation coefficient (r), several models were indistinguishable, namely the A2, A3, A4, and F1 models. On the other hand, IM plots of desolvation data (Figures 8−10) show that the A3 model can be selected for both the tetrahydrofuran and dioxane solvates while the A2 model is the model of choice for the dioxolane solvate. Model selection is not as clear for the dioxane solvate as it is for tetrahydrofuran and dioxolane solvates. For dioxane, another model (P2) can also be selected because the isoconversional curve intersects E_a

TABLE 6: Fitted Kinetic Parameters for the Nonisothermal Desolvation of Sulfameter−Dioxane Solvate, Using the Coats−Redfern Method[a]

model	A (min^{-1})	E_a (kJ/mol)	r
A2	7.00×10^{16}	118.22	−0.9942[c]
A3[b]	4.03×10^{10}	76.84	−0.9939[c]
A4	2.82×10^{07}	56.14	−0.9935[c]
D1	3.74×10^{52}	362.15	−0.9623
D2	2.06×10^{57}	395.38	−0.9744
D3	2.93×10^{63}	440.35	−0.9871
D4	7.45×10^{58}	409.99	−0.9793
F1	2.19×10^{35}	242.38	−0.9945[c]
F2	2.33×10^{50}	341.57	−0.9858
F3	1.52×10^{69}	466.14	−0.9539
P2	7.66×10^{11}	86.09	−0.9585
P3	1.81×10^{07}	55.41	−0.9556
P4	8.12×10^{04}	40.07	−0.9523
R1	3.52×10^{25}	178.11	−0.9611
R2	3.33×10^{29}	206.12	−0.9812
R3	1.08×10^{31}	217.21	−0.9867

*Results averaged from five curves by taking the geometrical mean of A and E_a and arithmetic mean of r. [b] Model selected based on isoconversional-model (IM) plots. [c] Equivalent models based on goodness of fit.

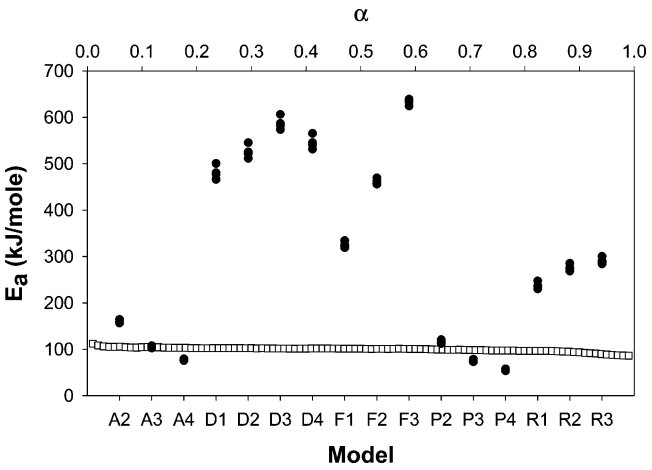

Figure 8. Isoconversional-model plot of activation energies for the nonisothermal desolvation of sulfameter−tetrahydrofuran solvate calculated by (●) Coats−Redfern's modelistic method and (□) Vyazovkin's isoconversional method.

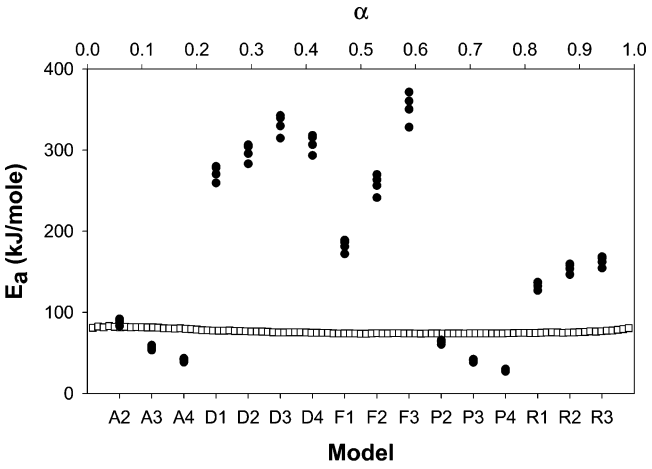

Figure 9. Isoconversional-model plot of activation energies for the nonisothermal desolvation of sulfameter−dioxolane solvate calculated by (●) Coats−Redfern's modelistic method and (□) Vyazovkin's isoconversional method.

values for both the A3 and P2 models (Figure 10). This could be due to small variations in the isoconversional curve as the reaction progresses or because these models are mechanistically

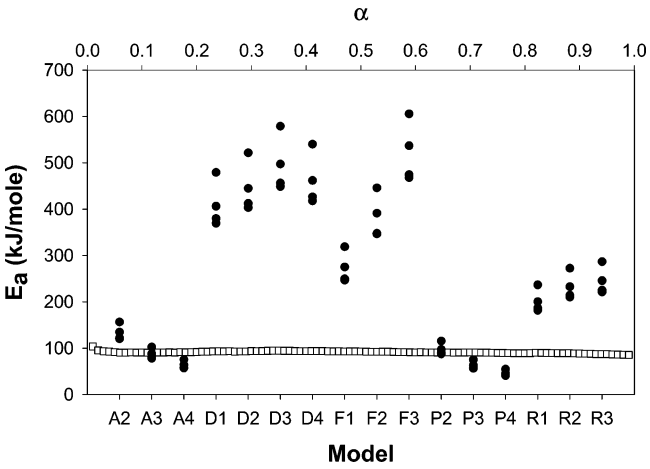

Figure 10. Isoconversional-model plot of activation energies for the nonisothermal desolvation of sulfameter−dioxane solvate calculated by (●) Coats−Redfern's modelistic method and (□) Vyazovkin's isoconversional method.

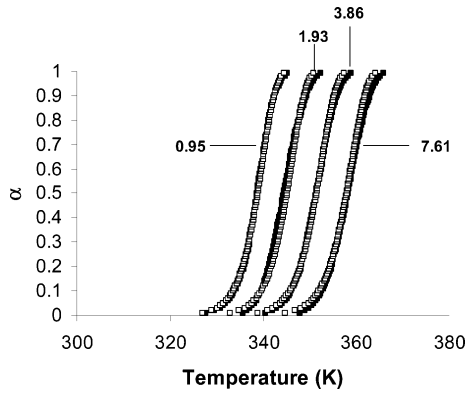

Figure 11. Reconstructed α−T plots for nonisothermal desolvation of sulfameter−tetrahydrofuran solvate for four heating rates (0.95, 1.93, 3.86, and 7.61 K/min): (■) experimental curves and (□) reconstructed curves (A3).

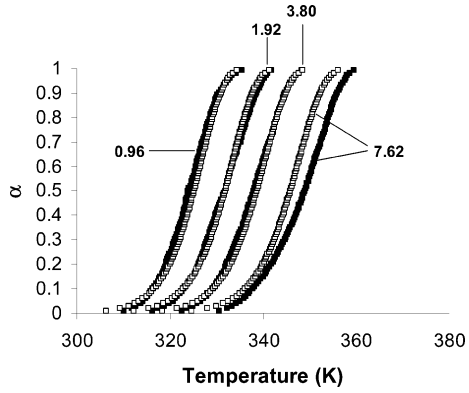

Figure 12. Reconstructed α−T plots for nonisothermal desolvation of sulfameter−dioxolane solvate for four heating rates (0.96, 1.92, 3.80, and 7.62 K/min): (□) experimental curves and (□) reconstructed curves (A2).

similar (i.e. both are nucleation models), which in turn results in similar values of E_a. To better judge which is the most accurate model, TGA curve reconstructions from E_a and A values for both models were conducted and compared.

Figures 11−13 show reconstructed $\alpha-T$ plots for the nonisothermal desolvation of the different sulfameter solvates. For each solvate, the kinetic triplet (A, E_a, and model) was selected based on isoconversional-model plots (Figures 8−10). There is good correlation between the reconstructed and actual experimental

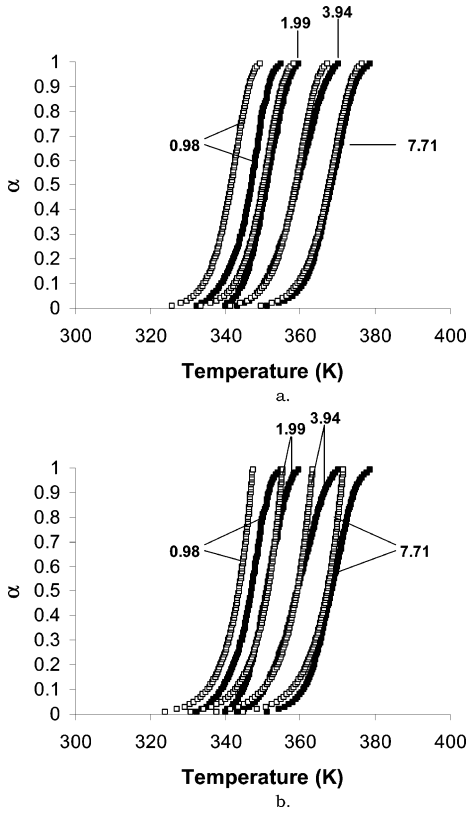

Figure 13. Reconstructed α−T plots for nonisothermal desolvation of sulfameter−dioxane solvate for four different heating rates (0.98, 1.99, 3.94, and 7.71 K/min): (■) experimental curves and (□) reconstructed curves (a, A3; b, P2).

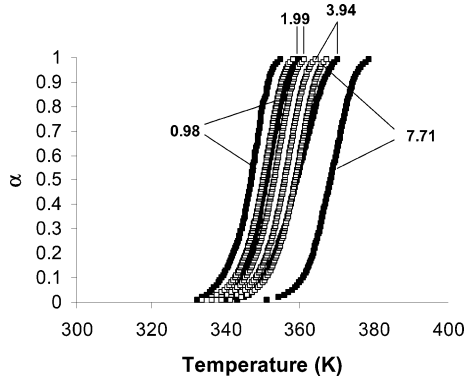

Figure 14. Reconstructed α−T plots for nonisothermal desolvation of sulfameter−dioxane solvate for four heating rates (0.98, 1.99, 3.94, and 7.71 K/min): (■) experimental curves and (□) reconstructed curves (F1).

data in most cases. In some cases, there is less correlation between reconstructed and experimental curves which may be due to using average values of E_a and A from the Coats and Redfern analysis. Figure 13 shows reconstructed α−*T* plots for the nonisothermal desolvation of the dioxane solvate for two models, A3 (Figure 13a) and P2 (Figure 13b). It is clear that the A3 model accurately predicts while the P2 model less accurately predicts experimental curves, especially at $\alpha > 0.5$.

If a mechanistic model is selected based on the correlation coefficient, the model of choice for the dioxane solvate (Table 6) would be a first-order (F1) model. However, when α−*T* curves are reconstructed with the F1 model, they poorly correlate with experimental α−*T* results, as seen in Figure 14. Therefore, such an approach is not satisfactory compared to model selection based on isoconversional methods.

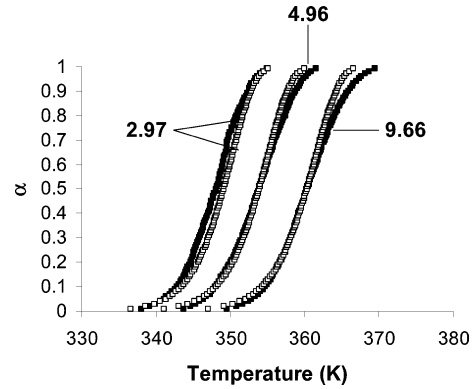

Figure 15. Predicted α−T plots for nonisothermal desolvation of sulfameter−tetrahydrofuran solvate at three heating rates (2.97, 4.96, and 9.66 K/min): (■) experimental and (□) predicted (A3).

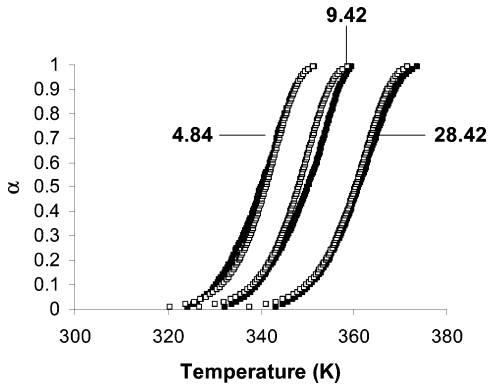

Figure 16. Predicted α−T plots for the nonisothermal desolvation of sulfameter−dioxolane solvate at three heating rates (4.84, 9.42, and 28.42 K/min): (■) experimental and (□) predicted (A2).

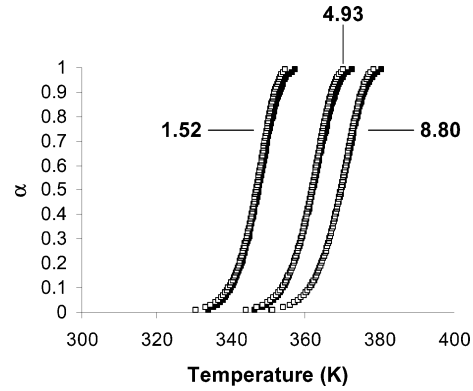

Figure 17. Predicted α−T plots for the nonisothermal desolvation of sulfameter−dioxane solvate at three heating rates (1.52, 4.93, and 8.80 K/min): (■) experimental and (□) predicted (A3).

Figures 15−17 show predicted and experimental α−*T* plots for the nonisothermal desolvation of sulfameter solvates. These plots show that nonisothermal curves have been reasonably well predicted from the kinetic triplet (A, E_a, and model). These results also agree with those of Caira and Mohamed [29] for the tetrahydrofuran solvate where they reported an activation energy of 103 kJ/mol by a model-independent method, which is similar to the value of 104.5 kJ/mol we obtained for the same solvate.

Although kinetic parameters needed to characterize the desolvation reactions were obtained, general mechanistic conclusions about sulfameter solvate desolvation cannot be drawn due to the limited number of solvates studied. Through the study of more such sulfameter solvates we hope that a correlation of kinetic parameters with solvent structure/size will emerge.

4. Conclusions

The large number of methods for evaluating solid-state kinetics has created some debate over the appropriate method or group of methods that should be used for analyzing such data. Different kinetic analysis methods have been treated by some investigators as competing rather than complementary. The increasing popularity of isoconversional methods has been at the expense of model-fitting methods. However, to fully study any kinetic process, it should be adequately described by a kinetic triplet (A, E_a, and model), which is not directly obtained from isoconversional methods. Yet, model-fitting methods suffer from severe shortcomings that limit their sole use for analyzing and understanding solid-state reactions.

Kinetic analysis of simulated data, in addition to that for the desolvation of sulfameter solvates, has shown that, selecting a model based on statistical methods using a common model-fitting method (i.e., Coats and Redfern) can produce misleading results, as shown by other investigators.[4,20]

Our approach combines the power of isoconversional and model-fitting methods for the evaluation of solid-state kinetics. This has produced promising results for simulated and real experimental data but, as with any kinetic method, this approach has some limitations. One is the assumption of a simple reaction or a flat isoconversional plot (i.e., constant activation energy throughout the reaction). This assumption seems to be applicable to the sulfameter−solvate system where solvent molecules fill channels within the crystal structure and desolvation involves the removal of solvent from such channels.[29] This approach is also not applicable to isothermal experiments where different models yield comparable values of the activation energy. The success of this approach also depends on careful control of experimental variables because poorly executed experimental protocols can lead to inaccurate isoconversional results which in turn can lead to inappropriate model selection. One must be able to carefully and reproducibly generate TGA data for accurate comparison of results at different heating rates.[2] When more than one model is selected with this approach, $\alpha - T$ curve reconstruction can be further used to select the most appropriate model.

Results from both modelistic and model-free approaches have been separately reported and compared in the literature.[30−32] Our approach represents a complementary means for using the strengths of both methods in the evaluation of solid-state kinetics.

References and Notes

(1) Khawam, A.; Flanagan, D. R. *Thermochim. Acta* **2005**, *429*, 93.

(2) Khawam, A.; Flanagan, D. R. *Thermochim. Acta* **2005**, submitted for publication.

(3) Zhou, D. L.; Grant, D. J. W. *J. Phys. Chem. A* **2004**, *108*, 4239.

(4) Vyazovkin, S.; Wight, C. A. *J. Phys. Chem. A* **1997**, *101*, 8279.

(5) Maciejewski, M.; Reller, A. *Thermochim. Acta* **1987**, *110*, 145.

(6) Maciejewski, M. *Thermochim. Acta* **2000**, *355*, 145.

(7) Sewry, J. D.; Brown, M. E. *Thermochim. Acta* **2002**, *390*, 217.

(8) Laidler, K. J. *J. Chem. Educ.* **1984**, *61*, 494.

(9) Flynn, J. H. *Thermochim. Acta* **1997**, *300*, 83.

(10) Doyle, C. D. *Nature* **1965**, *207*, 290.

(11) Doyle, C. D. *J. Appl. Polym. Sci.* **1962**, *6*, 639.

(12) Doyle, C. D. *J. Appl. Polym. Sci.* **1961**, *5*, 285.

(13) Senum, G. I.; R. T. Yang. *J. Therm. Anal.* **1977**, *11*, 445.

(14) Coats, A. W.; Redfern, J. P. *Nature* **1964**, *201*, 68.

(15) Coats, A. W.; Redfern, J. P. *J. Polym. Sci., Part B*: *Polym. Lett.* **1965**, *3*, 917.

(16) Brown, M. E.; Maciejewski, M.; Vyazovkin, S.; Nomen, R.; Sempere, J.; Burnham, A.; Opfermann, J.; Strey, R.; Anderson, H. L.; Kemmler, A.; Keuleers, R.; Janssens, J.; Desseyn, H. O.; Li, C. R.; Tang, T. B.; Roduit, B.; Malek, J.; Mitsuhashi, T. *Thermochim. Acta* **2000**, *355*, 125.

(17) Vyazovkin, S. *Thermochim. Acta* **2000**, *355*, 155.

(18) Burnham, A. K. *Thermochim. Acta* **2000**, *355*, 165.

(19) Roduit, B. *Thermochim. Acta* **2000**, *355*, 171.

(20) Vyazovkin, S.; Wight, C. A. *Int. Rev. Phys. Chem.* **1998**, *17*, 407.

(21) Bolton, S. *Pharmaceutical statistics*: *practical and clinical applications*, 1st ed.; Dekker: New York, 1984; p 188.

(22) Tang, T. B.; Chaudhri, M. M. *J. Therm. Anal.* **1980**, *18*, 247.

(23) Gao, X.; Chen, D.; Dollimore, D. *Thermochim. Acta* **1993**, *223*, 75.

(24) Vyazovkin, S.; Dollimore, D. *J. Chem. Inf. Comput. Sci.* **1996**, *36*, 42.

(25) Vyazovkin, S. *Int. J. Chem. Kinet.* **1996**, *28*, 95.

(26) Galwey, A. K.; Brown, M. E. *Thermochim. Acta* **1997**, *300*, 107.

(27) Byrn, S. R.; Pfeiffer, R. R.; Stowell, J. G. *Solid-State Chemistry of Drugs*, 2nd ed.; SSCI Inc.: West Lafayette, IN, 1999; p 279.

(28) Wilson, C. O.; Gisvold, O.; Doerge, R. F. *Textbook of Organic Medicinal and Pharmaceutical Chemistry*, 8th ed.; Lippincott: Philadelphia, PA, 1982; p 197.

(29) Caira, M. R.; Mohamed, R. *Supramol. Chem.* **1993**, *2*, 201.

(30) Dong, Z. D.; Salsbury, J. S.; Zhou, D. L.; Munson, E. J.; Schroeder, S. A.; Prakash, I.; Vyazovkin, S.; Wight, C. A.; Grant, D. J. W. *J. Pharm. Sci.* **2002**, *91*, 1423.

(31) Zhou, D. L.; Schmitt, E. A.; Zhang, G. G.; Law, D.; Vyazovkin, S.; Wight, C. A.; Grant, D. J. W. *J. Pharm. Sci.* **2003**, *92*, 1779.

(32) Zhou, D. L.; Schmitt, E. A.; Zhang, G. G. Z.; Law, D.; Wight, C. A.; Vyazovkin, S.; Grant, D. J. W. *J. Pharm. Sci.* **2003**, *92*, 1367.